

ARCI-causative genes (21, 25), its function in epidermal barrier formation has remained unsolved. Five missense mutations, all of which cause amino acid substitutions (F59L, R243H, R372W, H435Y, and H436D), have been found in the *CYP4F22* of patients with ichthyosis. To examine their role in ichthyosis pathology, we introduced these mutations into *CYP4F22* and examined the ω -hydroxylase activity of the resultant mutant proteins. All mutant proteins were expressed at levels equivalent to the wild-type protein (Fig. 3A), and indeed all ω -hydroxylase activity of the mutant *CYP4F22* proteins decreased to 4–20% of wild-type protein activity (Fig. 3B). Therefore, protein activity and ichthyosis pathology were nicely correlated.

Those points being noted, ichthyosis resulting from *CYP4F22* mutation is quite rare. In fact, only ~20 patients have been reported in Mediterranean populations (21), and only a single patient has been reported in Japan (25). The Japanese patient has compound heterozygous *CYP4F22* mutations: One is a point mutation (c.728G→A) causing an amino acid substitution (p.R243H; R243H), and the other is a deletion (c.1138delG) causing a frame shift (p.D380TfsX2; D380TfsX2) in which Asp380 is replaced by Thr followed by a stop codon (25). The mutant R243H exhibited decreased activity as described above (Fig. 3B). We also introduced the c.1138delG mutation into *CYP4F22* and examined the ω -hydroxylase activity of its truncated protein product. D380TfsX2 (predicted molecular mass, 44.8 kDa) migrated faster than the wild-type protein (62.0 kDa; Fig. 3A), and we found that it exhibited no activity (Fig. 3B).

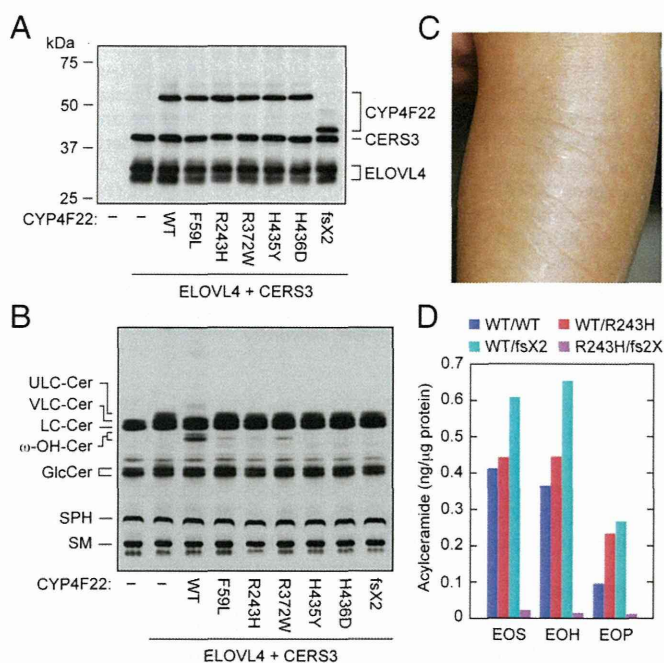


Fig. 3. Hydroxylase activity of *CYP4F22* is impaired by ichthyosis-causing mutations. (A and B) HEK 293T cells were transfected with plasmids encoding 3xFLAG-ELOVL4, 3xFLAG-CERS3, and 3xFLAG-CYP4F22 (wild type or mutant), as indicated. (A) Total cell lysates prepared from the transfected cells were separated by SDS/PAGE and subjected to immunoblotting with anti-FLAG antibodies. (B) The transfected cells were labeled with [³H]sphingosine for 4 h at 37 °C. Extracted lipids were separated by normal-phase TLC and detected by autoradiography. Cer, ceramide; GlcCer, glucosylceramide; SM, sphingomyelin; SPH, sphingosine; ω -OH, ω -hydroxy. (C) Representative clinical feature of a 2-y-old ARCI patient. Leaf-like flakes presented on the extensor side of the left lower limb before tape stripping. (D) Acylceramide (EOS, EOH, and EOP) levels in stratum corneum of a control (WT/WT), carriers (WT/R243H, the ichthyosis patient's father, and WT/D380Tfs2X (fs2X), the patient's mother), and an ARCI patient (R243H/D380T fs2X) were measured by LC-MS.

To confirm our conclusion that *CYP4F22* is involved in the production of acylceramide through ω -hydroxyceramide synthesis, we subjected the stratum corneum of the Japanese patient (Fig. 3C) and those of controls (her parents and a healthy volunteer) to LC-MS analysis and examined the levels of 11 major ceramide species. Although statistical analysis could not be performed because of the low number of samples, all three acylceramides containing sphingosine (EOS), 6-hydroxysphingosine (EOH), and phytosphingosine (EOP) were apparently decreased in the ARCI patient to one tenth of the levels in controls (Fig. 3D and Table S1). Instead, the nonacylated ceramides NS (which is a combination of sphingosine and a nonhydroxylated FA) and AS (which is a combination of sphingosine and an α -hydroxylated FA) seemed to be increased (Table S1). These results confirm that ω -hydroxyceramide production by *CYP4F22* is indeed required for acylceramide synthesis.

CYP4F22 Is a Type I Endoplasmic Reticulum Membrane Protein. We next examined the subcellular localization of *CYP4F22* by subjecting 3xFLAG-tagged *CYP4F22* to indirect immunofluorescence microscopy (Fig. 4A). 3xFLAG-CYP4F22 exhibited a reticular localization pattern and was colocalized with calnexin, HA-ELOVL4, and HA-CERS3, all of which are endoplasmic reticulum (ER) proteins, indicating that *CYP4F22* is localized in the ER. A hydrophathy plot showed that *CYP4F22* contains a highly hydrophobic region at the N terminus as well as some weak hydrophobic stretches (Fig. 4B). To reveal the membrane topology of *CYP4F22*, we introduced an N-glycosylation cassette, which is N-glycosylated when exposed to the lumen of the ER, into several positions of *CYP4F22*: the N terminus, E85/K (between Glu85 and Lys86 residues), H155/R, A285/L, C361/R, D455/N, and R508/K. Of these fusion proteins, only *CYP4F22* containing the N-glycosylation cassette at the N terminus received glycosylation, because the shift in molecular weight was observed upon treatment with endoglycosidase H (Fig. 4C). This result indicates that *CYP4F22* spans the ER membrane once. Furthermore, it oriented its N terminus to the ER lumen and oriented the large, hydrophilic C-terminal domain containing the active site to the cytosolic side of the ER membrane. The same membrane topology was determined for other CYP members by the detection of N-terminal N-glycosylation (26, 27).

When the N-terminal hydrophobic region was removed, the resulting *CYP4F22* Δ N became distributed throughout the cytoplasm (Fig. 4D). *CYP4F22* Δ N was fractionated into both soluble and membrane fractions by ultracentrifugation, in contrast to full-length *CYP4F22*, which was detected only in the membrane fraction (Fig. 4E). These results confirmed that *CYP4F22* is a type I ER membrane protein. *CYP4F22* Δ N could not produce ω -hydroxyceramide (Fig. 4F), suggesting that anchoring to the ER membrane, where all the reactions of acylceramide synthesis occur, is crucial for the *CYP4F22* function.

ULCFAs Are Substrates of *CYP4F22*. It was still unclear whether *CYP4F22* introduces an ω -hydroxyl group into ULCFAs before or after the formation of ceramide. Therefore, we examined ω -hydroxy FA levels using LC-MS in the presence of the ceramide synthase inhibitor fumonisin B₁. If ω -hydroxylation occurs before ceramide production, it was expected that free ω -hydroxy FA levels should be increased with fumonisin B₁ treatment. We found that ω -hydroxy FA levels with C26–C36 were increased significantly by the addition of fumonisin B₁ (Fig. 5A), suggesting that ω -hydroxylation occurs before ceramide production. Thus, it is highly likely that the substrates of *CYP4F22* are not ceramides but rather are FAs, the same type of substrate catalyzed by other *CYP4F* family members.

To confirm that the substrates of *CYP4F22* are FAs, we performed an in vitro analysis using yeast, which has no endogenous FA ω -hydroxylase activity. When C30:0 FA was used as a substrate,

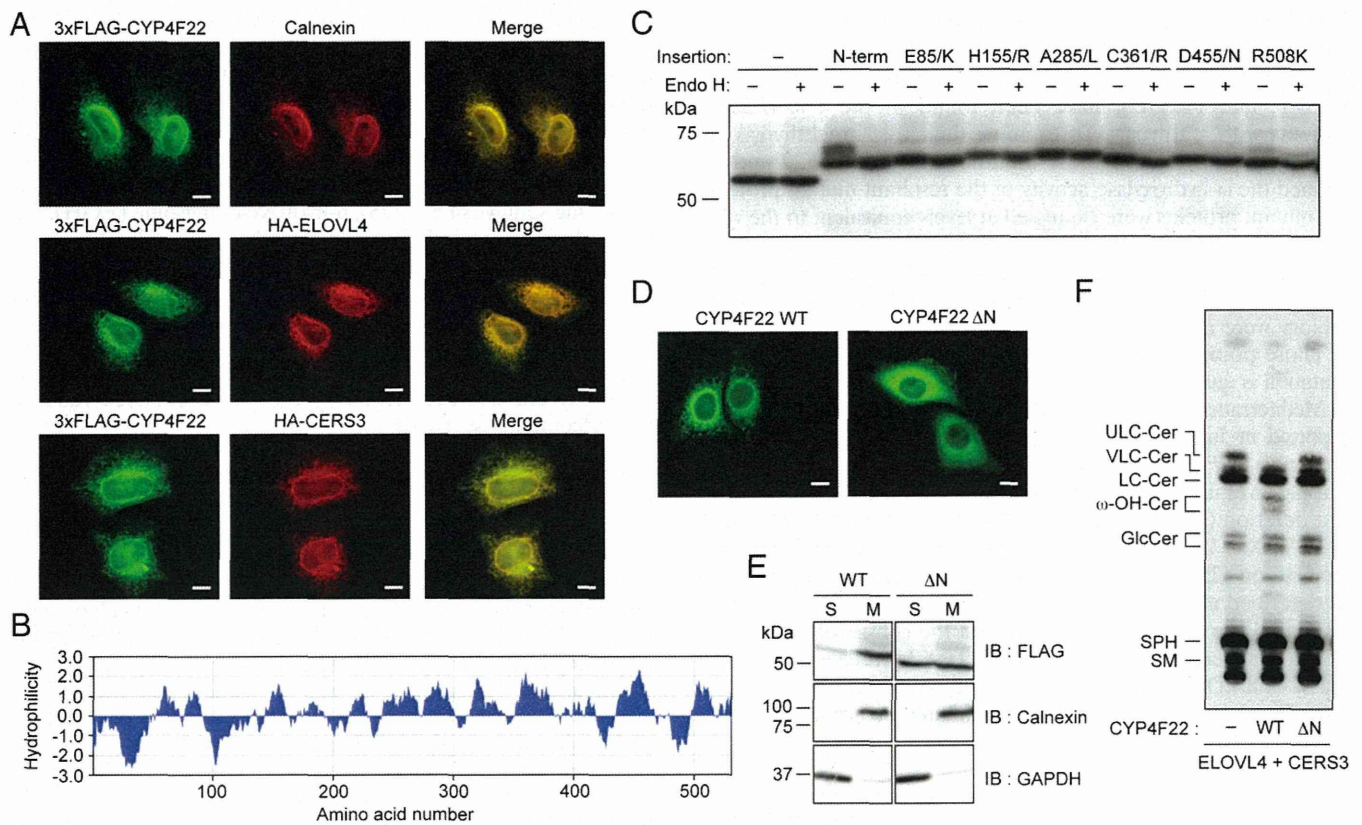


Fig. 4. CYP4F22 is a type I ER membrane protein. (A, D, and E) HeLa cells were transfected with plasmids encoding HA-ELOVL4, HA-CERS3, 3xFLAG-CYP4F22, and 3xFLAG-CYP4F22ΔN (CYP4F22 lacking 54 N-terminal amino acids), as indicated. (A and D) Cells were subjected to indirect immunofluorescence microscopic observation. (Scale bars, 10 μm.) (B) The hydrophobicity of CYP4F22 was analyzed by MacVector software (MacVector) using the Kyte and Doolittle algorithm (window size, 15). (C) HEK 293T cells were transfected with pCE-puro 3xFLAG-CYP4F22, pCE-puro 3xFLAG-CYP4F22 (N-term: insertion of the N-glycosylation cassette to the N terminus), pCE-puro 3xFLAG-CYP4F22 (E85/K: insertion of the cassette between Glu-85 and Lys-86), pCE-puro 3xFLAG-CYP4F22 (H155/R), pCE-puro 3xFLAG-CYP4F22 (A285/L), pCE-puro 3xFLAG-CYP4F22 (C361/R), pCE-puro 3xFLAG-CYP4F22 (D455/N), or pCE-puro 3xFLAG-CYP4F22 (R508/K). Lysates (3 μg) prepared from transfected cells were treated with or without endoglycosidase H (Endo H) and were separated by SDS/PAGE, followed by immunoblotting with anti-FLAG antibodies. (E) Total cell lysates (10 μg) were centrifuged at 100,000 × g for 30 min at 4 °C. The resulting supernatant (soluble fraction, S) and pellet (membrane fraction, M) were subjected to immunoblotting using anti-FLAG, anti-calnexin (membrane protein marker) or anti-GAPDH (soluble protein marker) antibodies. IB, immunoblotting. (F) HEK 293T cells transfected with plasmids encoding 3xFLAG-ELOVL4, 3xFLAG-CERS3, and 3xFLAG-CYP4F22 [wild type or CYP4F22ΔN (ΔN)], as indicated, were labeled with [³H]sphingosine for 4 h at 37 °C. Lipids were extracted, separated by normal-phase TLC, and detected by autoradiography. Cer, ceramide; GlcCer, glucosylceramide; SM, sphingomyelin; SPH, sphingosine; ω-OH, ω-hydroxy.

the total membrane fractions prepared from yeast bearing a vector plasmid exhibited FA ω-hydroxylase activity only at background levels (Fig. 5B). On the other hand, the ectopic expression of human CYP4F22 resulted in the production of ω-hydroxy FA in an NADPH-dependent manner (Fig. 5B). The hydroxylation reactions by CYP generally require O₂ and NADPH. These results indicated that the substrates of CYP4F22 are indeed FAs.

Acylceramide specifically contains ULCFA (mostly C28–C36) as its FA component. It is possible that the substrate preference of CYP4F22 determines the FA chain length of acylceramides. To examine this possibility, we prepared HEK 293T cells producing different sets of ceramides with specific chain lengths by introducing particular combinations of ceramide synthase and FA elongase (ELOVL1 and CERS2, C22–C24 ceramides; ELOVL1 and CERS3, C26 ceramide; and ELOVL4 and CERS3, ≥C26 ceramides) (Fig. 5C) (28, 29). Mammals have six ceramide synthases (CERS1–6) and seven FA elongases (ELOVL1–7), and each exhibits characteristic substrate specificity (Fig. S2B) (2, 4, 5, 28). When CYP4F22 was expressed in these cells producing different ceramide species, ω-hydroxyceramides were produced in cells producing C26 ceramide (ELOVL1/CERS3 combination) and ≥C26 ceramides (the ELOVL4/CERS3 combination) but not in cells producing C22–C24 ceramides (the ELOVL1/CERS2 combination) (Fig. 5D). These results suggest that CYP4F22 can

ω-hydroxylate ULCFAs (≥C26) but not VLCFAs (C22 and C24). The levels of ω-hydroxyceramide produced in ELOVL1/CERS3 cells were similar to those in ELOVL4/CERS3 cells, although the levels of nonhydroxyceramide substrates were much higher in ELOVL1/CERS3 cells (Fig. 5C). Thus, CYP4F22 exhibits especially high activity toward ULCFAs with ≥C28.

Discussion

Here we identified CYP4F22 as an ULCFA ω-hydroxylase involved in acylceramide production. Acylceramide is quite important for epidermal barrier formation, and impairment of its production (e.g. by ELOVL4 and CERS3 mutations) causes ichthyosis (15, 20). CYP4F22 was first identified as an ARCI-causative gene by Fischer and her coworkers (21). They proposed that CYP4F22 and most other ichthyosis-causative genes are involved in a metabolic pathway producing 12-lipoxygenase products (hepoxilins and trioxilins) from arachidonic acid by analogy to the 5-lipoxygenase pathway creating leukotrienes. In their scenario, arachidonic acid is first converted to 12(R)-hydroperoxyeicosatetraenoic acid [12(R)-HPETE] by one of the ichthyosis gene products, ALOX12B, and then to 12(R)-hepoxilin A₃ by another ichthyosis gene product, ALOXE3. 12(R)-Hepoxilin A₃ is further converted to a triol compound, 12(R)-trioxilin A₃. CYP4F22 was proposed to be involved in the metabolism of 12(R)-trioxilin A₃ by converting 12(R)-trioxilin A₃ to 20-hydroxy-

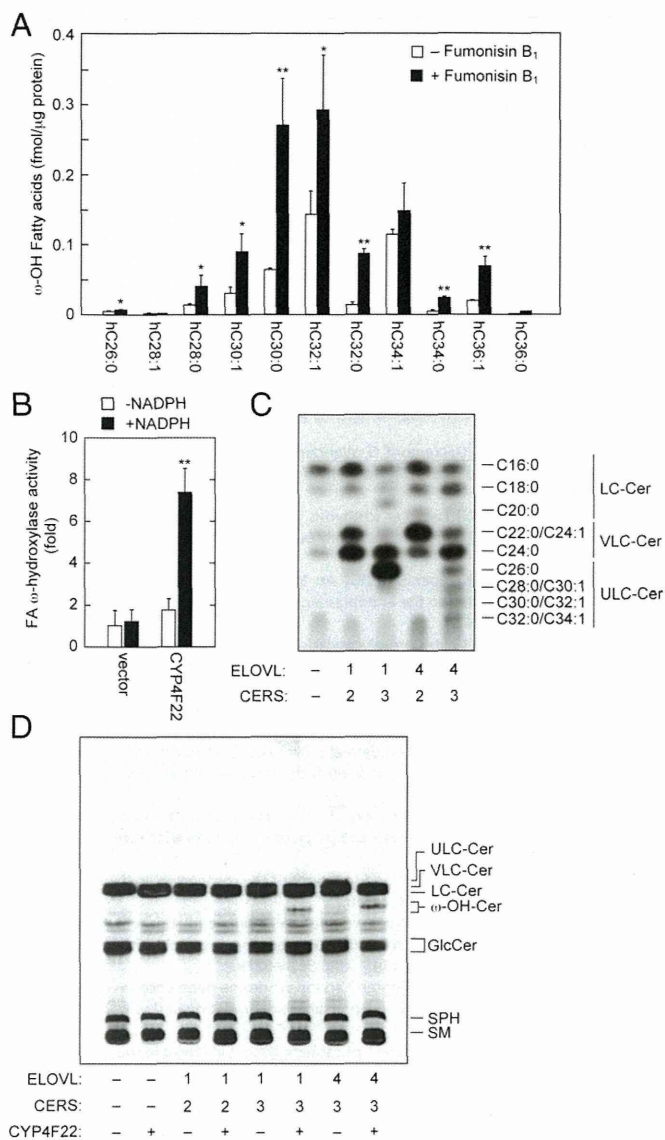


Fig. 5. CYP4F22 hydroxylates ULCFAs. (A) Keratinocytes were differentiated for 7 d in the presence or absence of 10 μ M fumonisin B₁. Lipids were extracted, treated with an alkali, and derivatized to AMPP amides. Derivatized FAs were analyzed by a Xevo TQ-S LC/MS system and quantified by MassLynx software. Statistically significant differences are indicated; * $P < 0.05$, ** $P < 0.01$; t test. hC26:0, hydroxy C26:0 FA. (B) Total membrane fractions (50 μ g) prepared from BY4741 bearing the pAK1017 (vector) or pNS29 (*His₆-Myc-3xFLAG-CYP4F22*) plasmids were incubated with 10 μ M C30:0 FA and 1 mM NADPH as indicated for 1 h at 37 °C. Lipids were extracted, derivatized to AMPP amides, and analyzed as in A. The values represent the amount of each FA ω -hydroxylase activity relative to that of the vector/-NADPH sample. The value of the CYP4F22/+NADPH sample was statistically different from the values of all other samples (** $P < 0.01$; t test). hC30:0, hydroxy C30:0 FA. (C and D) HEK 293T cells were transfected with the plasmids encoding *ELOVL1* or *ELOVL4*, *CERS2* or *CERS3*, and *CYP4F22*. Transfected cells were labeled with [³H]sphingosine for 4 h at 37 °C. Extracted lipids were separated by reverse-phase TLC (C) or by normal-phase TLC (D) and detected by autoradiography. Cer, ceramide; GlcCer, glucosylceramide; SM, sphingomyelin; SPH, sphingosine; ω -OH, ω -hydroxy.

12(*R*)-trioxilin A₃. However, the exact roles of hepxilins and trioxilins in epidermal barrier formation and/or keratinocyte differentiation are still unclear. Furthermore, recent findings have demonstrated that ALOX12B and ALOXE3 are involved in the reactions necessary for conversion of acylceramide to protein-

bound ceramide, i.e., peroxidation of the linoleate moiety and subsequent epoxyalcohol derivatization (13). In addition, ALOX12B was proven not to be involved in hepxilin/trioxilin production (30). These findings suggest that, although hepxilin/trioxilin metabolism may not be relevant to the pathogenesis of ichthyosis, the impairment of acylceramide/protein-bound ceramide formation causes ichthyosis. Based on these recent findings, some researchers have predicted that CYP4F22 is involved in acylceramide generation (3, 31), but until now their suppositions have lacked experimental evidence.

We determined the membrane topology of CYP4F22 (Fig. 4C), which indicates that the large C-terminal hydrophilic domain including catalytic residues is located in the cytosol. Therefore, ω -hydroxylation of the ULCFA portion of acylceramide must occur on the cytosolic side of the ER membrane. Based on this finding, we propose a working model for the process of acylceramide production in the ER membrane as follows (Fig. S6). Elongation of palmitoyl-CoA to ULCFA-CoA occurs on the cytoplasmic side of the ER membrane. Because lipids comprising the ER membrane are mostly C16 and C18, ULCFA (C28–C36) portions of ULCFA-CoAs should be bent in the cytosolic leaflet of the ER membrane (Fig. S6) or should penetrate into the luminal leaflet. Although the latter possibility cannot be excluded, we prefer the former, because in the latter model ULCFA must flip-flop at least three times in the ER membrane in the course of acylceramide production. Because the substrates of CYP4F22 are ULCFAs (Fig. 5), ULCFA-CoAs should be converted to ULCFAs before ω -hydroxylation. After ω -hydroxylation of ULCFAs by CYP4F22, the resulting ω -hydroxy-ULCFA is converted to ω -hydroxy-ULCFA-CoA by acyl-CoA synthetase. ACSVL4/FATP4 is the candidate acyl-CoA synthetase for this reaction, because *Acsvl4*-mutant mice exhibited skin barrier defects (32). CERS3 catalyzes the formation of ω -hydroxyceramide from ω -hydroxy-ULCFA-CoA and LCB. An unknown acyltransferase then introduces linoleic acid into the ω -hydroxy group of ω -hydroxyceramide, generating acylceramide.

Our results presented here demonstrate, for the first time to our knowledge, that CYP4F22 is a bona fide ULCFA ω -hydroxylase required for acylceramide production. Our findings provide important insights into the molecular mechanisms of skin permeability barrier formation. Future development of compounds that strengthen the skin permeability barrier by increasing acylceramide-synthetic proteins such as ELOVL4, CERS3, and CYP4F22 may be useful for treatment of cutaneous disorders including ichthyosis and atopic dermatitis.

Materials and Methods

Details of the materials and methods used for all procedures are given in *SI Materials and Methods*.

Ethics. Stratum corneum was obtained from an ARCI patient (a 2-y-old girl) (25), carriers (her parents) (mother, 35 y old, c.1138delG; father, 39 y old, c.728G→A), and a healthy control (an 11-y-old girl). This study was approved by the ethical committees of Nagoya University Graduate School of Medicine and the Kao Corporation. Informed consent was obtained from all participants after the procedures had been explained. Informed consents for the girls were obtained from their parents.

Plasmids. Human *CYP4F* subfamily genes and the human *CERS3* gene were amplified by PCR using their respective forward and reverse primers listed in Table S2. The amplified DNAs first were cloned into pGEM-T Easy Vector (Promega) and then were transferred to the pCE-puro 3xFLAG-1 plasmid, a mammalian expression vector designed to produce an N-terminal 3xFLAG-tagged protein.

[³H]Sphingosine Labeling Assay. Cells were labeled with 2 μ Ci [³-³H]sphingosine (20 Ci/mmol; PerkinElmer Life Sciences) for 4 h at 37 °C. Lipids were extracted as described previously (28, 33) and separated by normal-phase TLC and reverse-phase TLC.

Lipid Analysis Using LC-MS. FAs and ceramides prepared from cultured cells were analyzed by reversed-phase LC/MS using ultra-performance liquid chromatography (UPLC) coupled with electrospray ionization (ESI) tandem triple quadrupole MS (Xevo TQ-S; Waters). Each ceramide species was detected by multiple reaction monitoring (MRM) by selecting the *m/z* $[(M-H_2O+H)]^+$ and $[M+H]^+$ of specific ceramide species at Q1 and the *m/z* 264.2 at Q3 (Table S3). FAs were analyzed after derivatization to *N*-(4-aminomethylphenyl)pyridinium (AMPP) amides using the AMP⁺ Mass Spectrometry Kit (Cayman Chemical). Hydroxy FA species were detected by MRM by selecting the *m/z* $[M+H]^+$ of the derivatized hydroxy FA species at Q1 and the *m/z* 238.9 at Q3, corresponding to the fragment cleaved between C3 and C4 of derivatized FAs (Table S3). Stratum corneum ceramides were analyzed by reversed-phase LC/MS using the Agilent 1100 Series LC/MSD SL system (Agilent Technologies). Each ceramide species was detected by selected ion monitoring as *m/z* $[M+CH_3COO]^-$ (Table S4).

Immunoblotting. Immunoblotting was performed as described previously (34, 35) using anti-FLAG M2 (1.85 μ g/mL) (Sigma), anti-calnexin 4F10 (1 μ g/mL) (Medical & Biological Laboratories), or anti-GAPDH 6C5 (1 μ g/mL; Ambion, Life Technologies) antibody as a primary antibody and an HRP-conjugated anti-mouse IgG F(ab')₂ fragment (1:7,500 dilution; GE Healthcare Life Sciences) as a secondary antibody. Labeling was detected using Pierce ECL Western Blotting Substrate (Thermo Fisher Scientific).

ACKNOWLEDGMENTS. This work was supported by the Creation of Innovation Centers for Advanced Interdisciplinary Research Areas Program from the Ministry of Education, Culture, Sports, Science and Technology of Japan (A.K.); and Grant-in-Aid for Scientific Research (A) 26251010 (to A.K.) and Grant-in-Aid for Young Scientists (A) 15H05589 (to Y.O.), both from the Japan Society for the Promotion of Science.

- Uchida Y, Holleran WM (2008) Omega-O-acylceramide, a lipid essential for mammalian survival. *J Dermatol Sci* 51(2):77–87.
- Mizutani Y, Mitsutake S, Tsuji K, Kihara A, Igarashi Y (2009) Ceramide biosynthesis in keratinocyte and its role in skin function. *Biochimie* 91(6):784–790.
- Breiden B, Sandhoff K (2014) The role of sphingolipid metabolism in cutaneous permeability barrier formation. *Biochim Biophys Acta* 1841(3):441–452.
- Kihara A (2012) Very long-chain fatty acids: Elongation, physiology and related disorders. *J Biochem* 152(5):387–395.
- Sassa T, Kihara A (2014) Metabolism of very long-chain Fatty acids: Genes and pathophysiology. *Biomol Ther (Seoul)* 22(2):83–92.
- Farwanah H, Wohrlab J, Neubert RH, Raith K (2005) Profiling of human stratum corneum ceramides by means of normal phase LC/APCI-MS. *Anal Bioanal Chem* 383(4):632–637.
- Masukawa Y, et al. (2008) Characterization of overall ceramide species in human stratum corneum. *J Lipid Res* 49(7):1466–1476.
- Wertz PW, Cho ES, Downing DT (1983) Effect of essential fatty acid deficiency on the epidermal sphingolipids of the rat. *Biochim Biophys Acta* 753(3):350–355.
- Imokawa G, et al. (1991) Decreased level of ceramides in stratum corneum of atopic dermatitis: An etiologic factor in atopic dry skin? *J Invest Dermatol* 96(4):523–526.
- Ishikawa J, et al. (2010) Changes in the ceramide profile of atopic dermatitis patients. *J Invest Dermatol* 130(10):2511–2514.
- Janssens M, et al. (2012) Increase in short-chain ceramides correlates with an altered lipid organization and decreased barrier function in atopic eczema patients. *J Lipid Res* 53(12):2755–2766.
- Wertz PW, Downing DT (1987) Covalently bound ω -hydroxyacylsphingosine in the stratum corneum. *Biochim Biophys Acta* 917(1):108–111.
- Zheng Y, et al. (2011) Lipoxygenases mediate the effect of essential fatty acid in skin barrier formation: A proposed role in releasing omega-hydroxyceramide for construction of the corneocyte lipid envelope. *J Biol Chem* 286(27):24046–24056.
- Jobard F, et al. (2002) Lipoxygenase-3 (ALOXE3) and 12(R)-lipoxygenase (ALOX12B) are mutated in non-bullous congenital ichthyosiform erythroderma (NCIE) linked to chromosome 17p13.1. *Hum Mol Genet* 11(1):107–113.
- Eckl KM, et al. (2013) Impaired epidermal ceramide synthesis causes autosomal recessive congenital ichthyosis and reveals the importance of ceramide acyl chain length. *J Invest Dermatol* 133(9):2202–2211.
- Traupe H, Fischer J, Oji V (2014) Nonsyndromic types of ichthyoses - an update. *J Dtsch Dermatol Ges* 12(2):109–121.
- Jennemann R, et al. (2012) Loss of ceramide synthase 3 causes lethal skin barrier disruption. *Hum Mol Genet* 21(3):586–608.
- Krieg P, Fürstenberger G (2014) The role of lipoxygenases in epidermis. *Biochim Biophys Acta* 1841(3):390–400.
- Akiyama M, Shimizu H (2008) An update on molecular aspects of the non-syndromic ichthyoses. *Exp Dermatol* 17(5):373–382.
- Aldahmesh MA, et al. (2011) Recessive mutations in ELOVL4 cause ichthyosis, intellectual disability, and spastic quadriplegia. *Am J Hum Genet* 89(6):745–750.
- Lefèvre C, et al. (2006) Mutations in a new cytochrome P450 gene in lamellar ichthyosis type 3. *Hum Mol Genet* 15(5):767–776.
- Behne M, et al. (2000) Omega-hydroxyceramides are required for corneocyte lipid envelope (CLE) formation and normal epidermal permeability barrier function. *J Invest Dermatol* 114(1):185–192.
- Dhar M, Sepkovic DW, Hirani V, Magnusson RP, Lasker JM (2008) Omega oxidation of 3-hydroxy fatty acids by the human CYP4F gene subfamily enzyme CYP4F11. *J Lipid Res* 49(3):612–624.
- Sanders RJ, Ofman R, Dacremont G, Wanders RJ, Kemp S (2008) Characterization of the human ω -oxidation pathway for ω -hydroxy-very-long-chain fatty acids. *FASEB J* 22(6):2064–2071.
- Sugiura K, et al. (2013) Lamellar ichthyosis in a collodion baby caused by CYP4F22 mutations in a non-consanguineous family outside the Mediterranean. *J Dermatol Sci* 72(2):193–195.
- Szczesna-Skorupa E, Kemper B (1993) An N-terminal glycosylation signal on cytochrome P450 is restricted to the endoplasmic reticulum in a luminal orientation. *J Biol Chem* 268(3):1757–1762.
- Shimozawa O, et al. (1993) Core glycosylation of cytochrome P-450(arom). Evidence for localization of N terminus of microsomal cytochrome P-450 in the lumen. *J Biol Chem* 268(28):21399–21402.
- Ohno Y, et al. (2010) ELOVL1 production of C24 acyl-CoAs is linked to C24 sphingolipid synthesis. *Proc Natl Acad Sci USA* 107(43):18439–18444.
- Sassa T, et al. (2013) Impaired epidermal permeability barrier in mice lacking *elov1*, the gene responsible for very-long-chain fatty acid production. *Mol Cell Biol* 33(14):2787–2796.
- Krieg P, et al. (2013) *Aloxe3* knockout mice reveal a function of epidermal lipoxygenase-3 as hepxoxilin synthase and its pivotal role in barrier formation. *J Invest Dermatol* 133(1):172–180.
- Elias PM, et al. (2014) Formation and functions of the corneocyte lipid envelope (CLE). *Biochim Biophys Acta* 1841(3):314–318.
- Moulson CL, et al. (2003) Cloning of wrinkle-free, a previously uncharacterized mouse mutation, reveals crucial roles for fatty acid transport protein 4 in skin and hair development. *Proc Natl Acad Sci USA* 100(9):5274–5279.
- Nakahara K, et al. (2012) The Sjögren-Larsson syndrome gene encodes a hexadecenal dehydrogenase of the sphingosine 1-phosphate degradation pathway. *Mol Cell* 46(4):461–471.
- Kihara A, et al. (2003) Sphingosine-1-phosphate lyase is involved in the differentiation of F9 embryonal carcinoma cells to primitive endoderm. *J Biol Chem* 278(16):14578–14585.
- Kitamura T, Takagi S, Naganuma T, Kihara A (2015) Mouse aldehyde dehydrogenase ALDH3B2 is localized to lipid droplets via two C-terminal tryptophan residues and lipid modification. *Biochem J* 465(1):79–87.
- Brachmann CB, et al. (1998) Designer deletion strains derived from *Saccharomyces cerevisiae* S288C: A useful set of strains and plasmids for PCR-mediated gene disruption and other applications. *Yeast* 14(2):115–132.
- Kihara A, Sakuraba H, Ikeda M, Denpoh A, Igarashi Y (2008) Membrane topology and essential amino acid residues of Phs1, a 3-hydroxyacyl-CoA dehydratase involved in very long-chain fatty acid elongation. *J Biol Chem* 283(17):11199–11209.
- Vasireddy V, et al. (2007) Loss of functional ELOVL4 depletes very long-chain fatty acids (\geq C28) and the unique ω -O-acylceramides in skin leading to neonatal death. *Hum Mol Genet* 16(5):471–482.
- Ogawa C, Kihara A, Gokoh M, Igarashi Y (2003) Identification and characterization of a novel human sphingosine-1-phosphate phosphohydrolase, hSP2. *J Biol Chem* 278(2):1268–1272.
- Kondo N, et al. (2014) Identification of the phytosphingosine metabolic pathway leading to odd-numbered fatty acids. *Nat Commun* 5:5338.

Supporting Information

Ohno et al. 10.1073/pnas.1503491112

SI Materials and Methods

Cell Culture and Transfection. HeLa and HEK 293T cells were cultured in DMEM (Sigma) supplemented with 10% FBS, 100 U/mL penicillin, and 100 μ g/mL streptomycin. HEK 293T cells were grown in dishes precoated with 0.3% collagen. Transfections were performed using Lipofectamine Reagent and Plus Reagent (Life Technologies), according to the manufacturer's protocols. Normal human epidermal keratinocytes isolated from juvenile donors were purchased from CELLnTEC and grown in PCT Epidermal Keratinocyte Medium (CELLnTEC). Keratinocyte differentiation was induced by exchanging the medium to Epidermal Keratinocyte 3D Prime Medium (CELLnTEC) after the cell confluency reached $\geq 80\%$.

The *Saccharomyces cerevisiae* strain BY4741 (*MATa his3 Δ 1 leu2 Δ 0 met15 Δ 0 ura3 Δ 0*) (36) was used. Cells were grown in synthetic complete (SC) medium (0.67% yeast nitrogen base and 2% D-glucose) containing 0.5% casamino acids, 20 mg/mL adenine, and 20 mg/mL tryptophan but lacking uracil (SC-URA).

Plasmids. The pCE-puro 3xFLAG-ELOVL4 plasmid encoding N-terminally 3xFLAG-tagged *ELOVL4* has been described previously (29). Human *CYP4F* subfamily genes and the human *CERS3* gene were amplified by PCR using their respective forward and reverse primers listed in Table S2. The amplified DNAs first were cloned into pGEM-T Easy Vector (Promega) and then were transferred to the pCE-puro 3xFLAG-1 plasmid, a mammalian expression vector designed to produce an N-terminal 3xFLAG-tagged protein. The *CYP4F22* gene was also transferred to the pAK1017 plasmid (*URA3* marker, *CEN*), a yeast expression vector designed to produce an N-terminal, tandemly oriented His₆-, Myc-, and 3xFLAG-tagged protein under the control of the *TDH3* (glyceraldehyde 3-phosphate dehydrogenase) promoter, creating the pNS29 plasmid. Ichthyosis mutations were introduced into the *CYP4F22* gene using the QuikChange Site-Directed Mutagenesis Kit (Agilent Technologies), using the primers described in Table S2. The N-glycosylation site cassette was inserted into the *CYP4F22* gene as described previously (37), using the T (topology)-series primers listed in Table S2.

[³H]Sphingosine Labeling Assay. HEK 293T cells were transfected with appropriate plasmids. Twenty-four hours after transfection, cells were labeled for 4 h at 37 °C with 2 μ Ci [³-³H]sphingosine (20 Ci/mmol; PerkinElmer Life Sciences). Cells were washed twice with 1 mL of PBS and suspended in 100 μ L of PBS. Lipids were extracted by successive addition and mixing of 375 μ L of chloroform/methanol/HCl (100:200:1, vol/vol/vol), 125 μ L of chloroform, and 125 μ L of 1% KCl. Phases were separated by centrifugation (20,000 \times g at room temperature for 3 min), after which the organic (lower) phase was recovered, dried, and subjected to normal-phase TLC (Silica Gel 60 TLC plates; Merck Millipore) with the following solvent systems: (i) chloroform/methanol/water (40:10:1, vol/vol/vol), developed to 2 cm from the bottom of the TLC plate, dried, and then developed again to 5 cm from the bottom; (ii) chloroform/methanol/acetic acid (47:2:0.5, vol/vol/vol), developed to the top; and (iii) hexane/diethylether/acetic acid (65:35:1, vol/vol/vol), developed to the top twice. Labeled lipids were visualized by spraying the plate with a fluorographic reagent [2.8 mg/mL 2,5-diphenyl-oxazole in 2-methylnaphthalene/1-butanol (1:3.3, vol/vol)]. The TLC plate was exposed to X-ray film at -80 °C.

For reverse-phase TLC analysis, extracted lipids were suspended in 150 μ L of 90% methanol and mixed with 150 μ L of

hexane. Methanol/water and hexane phases were separated by centrifugation, and the hexane (upper) phase was recovered. After hexane extraction was repeated three times, the extracted lipids were combined, dried, and suspended in chloroform/methanol (2:1, vol/vol). Lipids were separated by reverse-phase TLC with Silica Gel 60 RP-18 F254s TLC plates (Merck Millipore) with chloroform/methanol/water (15:15:2, vol/vol/vol) and detected as described above.

Lipid Analysis by MS. To examine ceramide and FA species prepared from cultured cells, lipids were analyzed by UPLC coupled with ESI tandem triple quadrupole MS (Xevo TQ-S; Waters). Cells were washed twice with 1 mL of PBS, suspended in 1 mL of PBS, and detached from culture dishes by pipetting. Cell suspensions were transferred to silicon-coated plastic tubes. After centrifugation (400 \times g at room temperature for 3 min), cells were suspended in 100 μ L of PBS, followed by the successive addition and mixing of 375 μ L of chloroform/methanol/12 M formic acid (100:200:1, vol/vol/vol), 2 μ L of 25 μ M C17:0 ceramide (internal standard; Avanti Polar Lipids), 125 μ L of chloroform, and 125 μ L of water. After centrifugation (9,000 \times g at room temperature for 1 min), the organic phase was recovered and dried. Lipids were suspended in 200 μ L of chloroform/methanol (1:2, vol/vol) and were mixed with 6 μ L of 4 M KOH. After incubation for 1 h at 37 °C, lipids were mixed with 7 μ L of 4 M formic acid, 66.6 μ L of chloroform, and 133.3 μ L of water. After centrifugation (9,000 \times g at room temperature for 1 min), the organic phase was recovered, dried, and dissolved in 50 μ L of chloroform/methanol (1:1, vol/vol). As controls, epidermal lipids were prepared from mice as described previously (29, 38). Lipids were resolved by UPLC on a reverse-phase column (ACQUITY UPLC BEH C18 column, length 150 mm; Waters) at 45 °C and were detected by MS. The flow rate was 0.1 mL/min in the binary gradient system using a mobile phase A [acetonitrile/water/methanol (4:4:2, vol/vol/vol) containing 0.1% formic acid and 0.025% ammonia] and a mobile phase B [2-propanol/methanol (4:1, vol/vol) containing 0.1% formic acid and 0.025% ammonia]. The elution gradient steps were as follows: 0 min, 5% B; 0–10 min, gradient to 60% B; 10–50 min, gradient to 80% B; 50–55 min, gradient to 100% B; 55–65 min, 100% B; 65–66 min, gradient to 5% B; 66–80 min, 5% B. The ESI capillary voltage was set at 3.0 kV; the sampling cone was set at 30 V; and the source offset was set at 50 V in positive ion mode. Each ceramide species was detected by MRM by selecting the m/z ([M–H₂O+H]⁺ and [M+H]⁺) of specific ceramide species at Q1 and the m/z 264.2 at Q3 (Table S3). Data analysis and quantification were performed using MassLynx software (Waters).

For quantitation of FAs in keratinocytes, lipids were extracted and treated with an alkali as described above. As an internal standard, C13:0 FA (0.2 pmol; Sigma) was added. Extracted lipids were dried, derivatized by an AMP⁺ Mass Spectrometry Kit (Cayman Chemical) according to the manufacturer's protocol, and resolved by UPLC-ESI MS essentially as described above except as outlined below. The flow rate was set at 0.15 mL/min and the elution gradient steps were set as follows: 0 min, 5% B; 0–3 min, gradient to 60% B; 3–10 min, gradient to 80% B; 10–11 min, gradient to 100% B; 11–20 min, 100% B; 20–21 min, gradient to 5% B; 21–30 min, 5% B. Hydroxy FA species were detected by MRM by selecting the m/z ([M+H]⁺) of the derivatized hydroxy FA species at Q1 and the m/z 238.9 at Q3, corresponding to the fragment cleaved between C3 and C4 of derivatized FAs (Table S3).

To examine ceramide species in the stratum corneum of human subjects, tape stripping was performed by pressing an acryl film tape

(465#40; Teraoka Seisakusho) to the skin of the forearm. Five strips, measuring 25 mm × 50 mm each, were obtained from a single person. The tapes were immersed in 3.0 mL methanol with 60 μL 500 nM C17:0 ceramide as an internal standard. After 10 min of sonication, the lipid extracts were dried under a nitrogen stream and then were dissolved in chloroform/methanol/2-propanol (10:45:45, vol/vol/vol) so that the final concentration of the internal standard was 50 nM. This lipid solution was subjected to reversed-phase LC/MS. An Agilent 1100 Series LC/MSD SL system equipped with a multi-ion source, ChemStation software, a 1,100-well plate autosampler (Agilent Technologies), and an L-column ODS (2.1 mm i.d. × 150 mm; Chemicals Evaluation and Research Institute) was used. Chromatographic separation of the lipids was achieved at a flow rate of 0.2 mL/min using a binary gradient solvent system of mobile phase C [methanol/ water (1:1, vol/vol) containing 5 mM acetic acid and 10 mM ammonium acetate] and mobile phase D (2-propanol containing 5 mM acetic acid and 10 mM ammonium acetate). The mobile phases were consecutively programmed as follows: 0–1 min, 20% D; 1–2 min, gradient to 60% D; 2–30 min, gradient to 100% D; 30–35 min, 100% D; 35–45 min, 20% D. The injection volume was 20 μL. The column temperature was maintained at 40 °C. Mass spectrometry parameters were as follows: polarity, negative ion mode; flow of heated dry nitrogen gas, 4.0 L/min; nebulizer gas pressure, 60 psi; heater temperature of nitrogen gas, 350 °C; vaporizer temperature, 200 °C; capillary voltage, 4,000 V; charging voltage, 2,000 V; fragmenter voltage, 200 V. Each ceramide species was detected by selected ion monitoring as m/z $[M+CH_3COO]^-$ (Table S4).

Immunofluorescence Microscopy. Indirect immunofluorescence microscopy was performed essentially as described previously

(39), using anti-FLAG M2 (10 μg/mL; Sigma), anti-calnexin 4F10 (10 μg/mL; Medical & Biological Laboratories), or anti-HA HA-7 (50 μg/mL; Sigma) antibody as a primary antibody and Alexa Fluor 488-conjugated anti-rabbit antibody or Alexa Fluor 594-conjugated anti-mouse antibody (each at 5 μg/mL; Molecular Probes, Life Technologies) as a secondary antibody. Coverslips were mounted with Prolong Gold Antifade Reagent (Molecular Probes, Life Technologies) and observed under a Leica DM5000B microscope (Leica Microsystems).

Deglycosylation. Protein deglycosylation was performed using endoglycosidase H (New England Biolabs), according to the manufacturer's instructions.

In Vitro FA ω-Hydroxylase Assay. Total membrane fractions were prepared from yeast cells as described previously (40) and were suspended in assay buffer [100 mM potassium phosphate (pH 7.4), 10% glycerol, 1× Complete protease inhibitor mixture (EDTA-free; Roche Diagnostics), 1 mM phenylmethylsulfonyl fluoride, and 1 mM DTT]. The substrate C30:0 FA (1 mM, 0.5 μL; Tokyo Chemical Industry) was dissolved in chloroform, aliquoted into plastic tubes, dried, and then suspended in a mixture of 25 μL of yeast membrane fractions (50 μg protein), 23 μL of assay buffer, and 1 μL of 10% digitonin by sonication. After addition of 1 μL of 50 mM NADPH or water, samples were incubated for 1 h at 37 °C. Lipids were extracted by the successive addition and mixing of 33.15 μL of 5 M HCl, 91.85 μL of water, 100 μL of ethanol, and 700 μL of hexane. After centrifugation, the organic phase was recovered, dried, derivatized by an AMP⁺ Mass Spectrometry Kit, and resolved by UPLC-ESI MS, as described above.

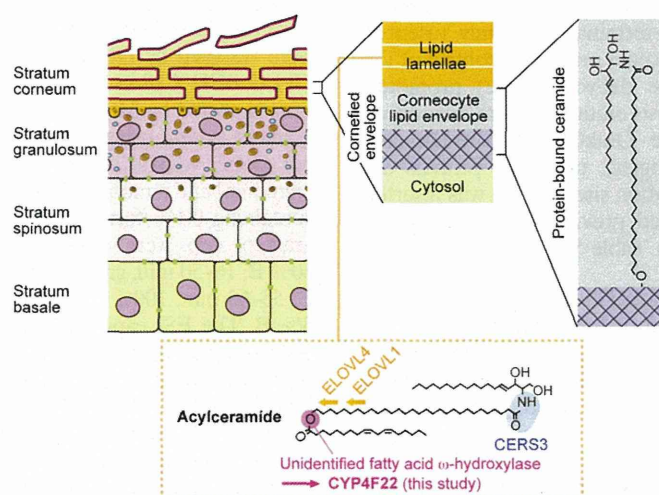
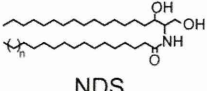
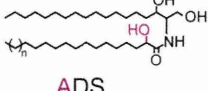
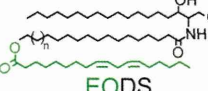
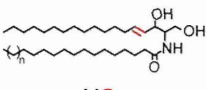
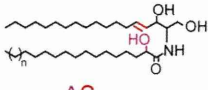
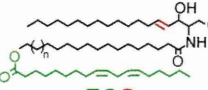
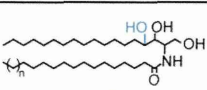
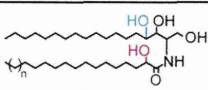
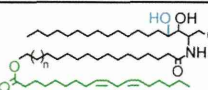
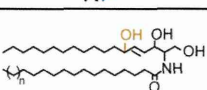
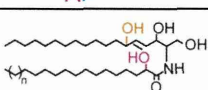
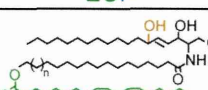


Fig. S1. Structures of the epidermis, the stratum corneum, acylceramide, and protein-bound ceramide. Acylceramides are produced mainly in the stratum granulosum and partly in the stratum spinosum and are stored in lamellar bodies as glucosylated forms (acyl glucosylceramides). At the interface of the stratum granulosum and stratum corneum, the lamellar bodies fuse with the plasma membrane and release their contents into the extracellular space, where acyl glucosylceramides are converted to acylceramides. Thus, released acylceramides, FAs, and cholesterol form lipid lamellae in the stratum corneum. Some acylceramide is hydrolyzed to ω-hydroxyceramide, followed by covalent binding to corneocyte surface proteins to create corneocyte lipid envelopes. Acylceramide contains ULCFAs with carbon chain lengths of C28–C36. The FA elongase ELOVL1 produces VLCFAs, which are further elongated to ULCFAs by ELOVL4 (29). The ceramide synthase CERS3 creates an amide bond between ULCFAs and LCB (17). ω-Hydroxylation of ULCFAs is required for acylceramide production. However, the responsible ω-hydroxylase had not been identified previously; its identification is the subject of this research.

A

LCBs \ FAs	Non-hydroxy FA [N]	α -hydroxy FA [A]	Esterified ω -hydroxy FA [EO]
Dihydrosphingosine [DS]	 NDS	 ADS	 EODS
Sphingosine [S]	 NS	 AS	 EOS
Phytosphingosine [P]	 NP	 AP	 EOP
6-Hydroxysphingosine [H]	 NH	 AH	 EOH

B

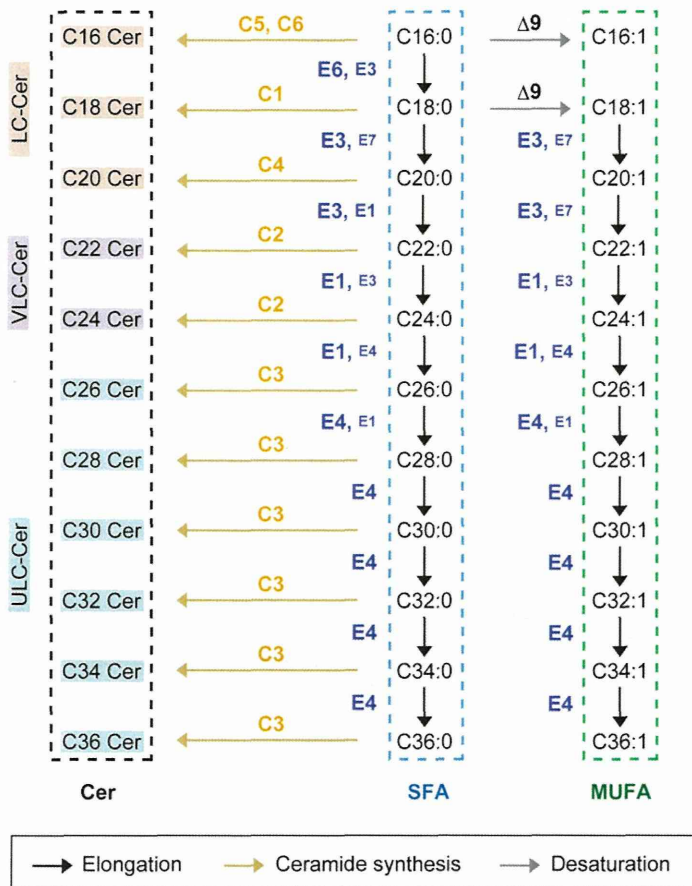


Fig. S2. Structure and synthetic pathways of ceramides in mammals. (A) Structure and nomenclature of epidermal ceramides. Epidermal ceramides are classified into 12 classes depending on their differences in the LCB and FA moieties. N-type and A-type ceramides contain C16–C30 FAs ($n = 1-15$), whereas EO-type ceramides contain C28–C36 FAs ($n = 13-21$) (6, 7). (B) FA elongation and ceramide synthesis in mammals. The FA elongation pathways of saturated and monounsaturated FAs and the ceramide-synthetic pathways are illustrated. E1–E7 and C1–C6 indicate the ELOVL (ELOVL1–7) and CERS (CERS1–6) isozymes involved in each step, respectively. The differences in the letter size of E1–E7 reflect their enzyme activities in each FA elongation reaction. Cer, ceramide; MUFA, monounsaturated FA; SFA, saturated FA.

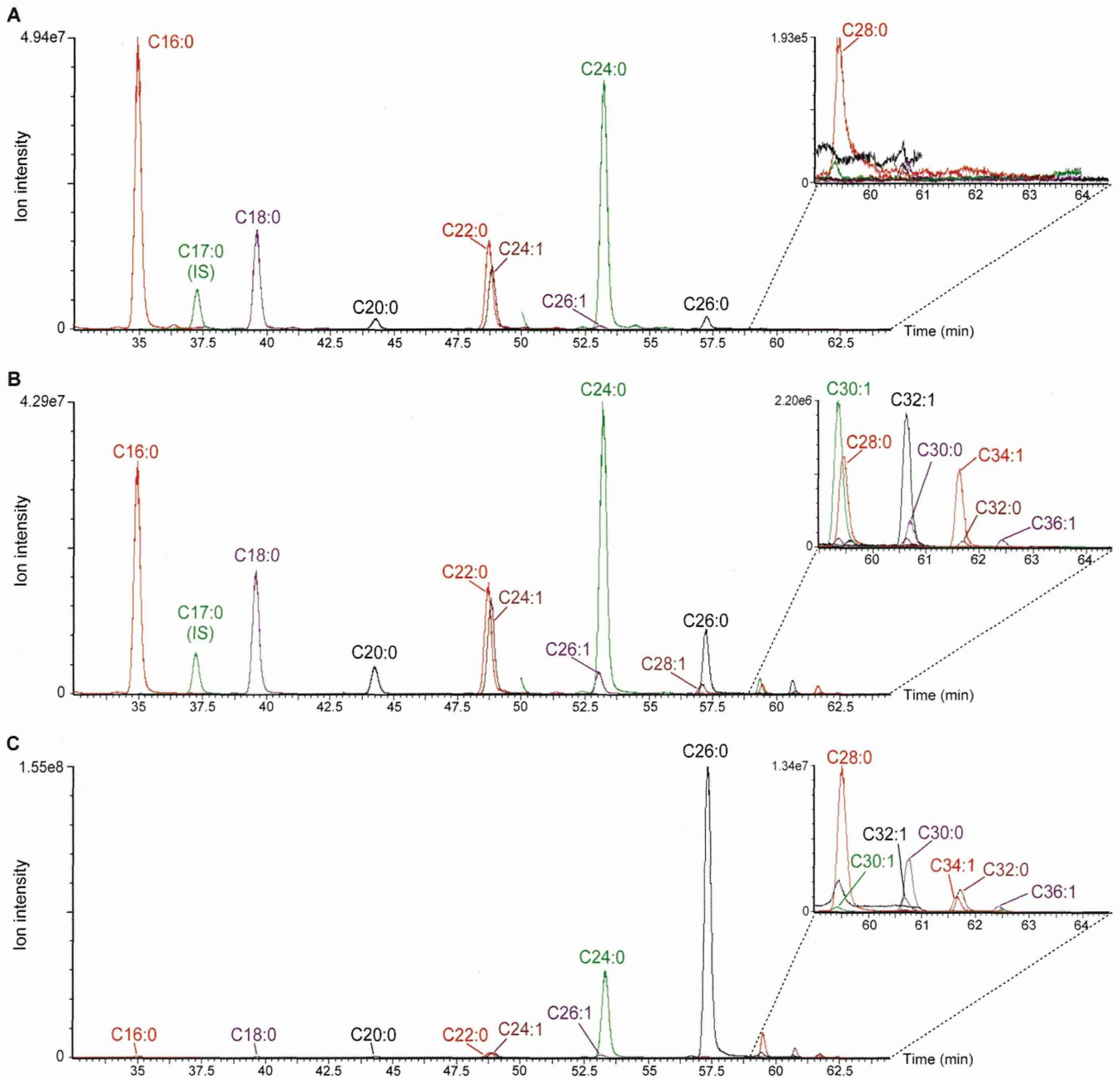


Fig. S3. MRM chromatogram of ceramides produced by combined ELOVL4 and CERS3 expression. Lipids were extracted from HEK 293T cells transfected with control vector (A) or pCE-puro 3xFLAG-ELOVL4 and pCE-puro 3xFLAG-CERS3 (B) or mouse epidermis (C) and subjected to UPLC/ESI-MS using a triple quadrupole mass spectrometer (Xevo TQ-S; Waters). Each ceramide was detected by MRM by setting the appropriate $[M+H]^+$ and $[M+H-H_2O]^+$ values at Q1 and m/z 264.2 (corresponding to C18:0 sphingosine) at Q3. Each MRM peak was overlaid using MassLynx software. *Insets* show enlarged views of the indicated areas of the original chromatograms.

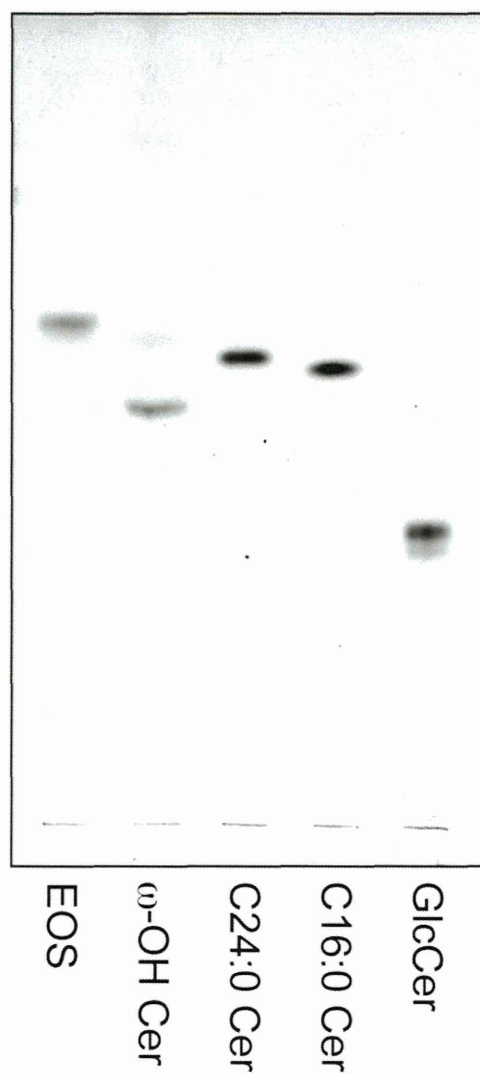


Fig. S4. TLC chromatogram of ceramides. The acylceramide EOS and ω -hydroxyceramide were prepared as follows. Lipids were prepared from mouse epidermis and separated by normal-phase TLC. Silica containing EOS ceramide was scraped from the TLC plate and eluted with chloroform/methanol (1:2, vol/vol). A portion of EOS ceramide was converted to ω -hydroxyceramide by hydrolysis of the ester bond connecting ω -hydroxyceramide and linoleic acid with 0.1 M NaOH. The prepared EOS ceramide and ω -hydroxyceramide, as well as C24:0 ceramide (Avanti Polar Lipids), C16:0 ceramide (Avanti Polar Lipids), and glucosylceramide (Avanti Polar Lipids), were separated by normal-phase TLC and visualized by cupric acetate/phosphoric acid staining. Cer, ceramide; GlcCer, glucosylceramide; ω -OH Cer, ω -hydroxyceramide.

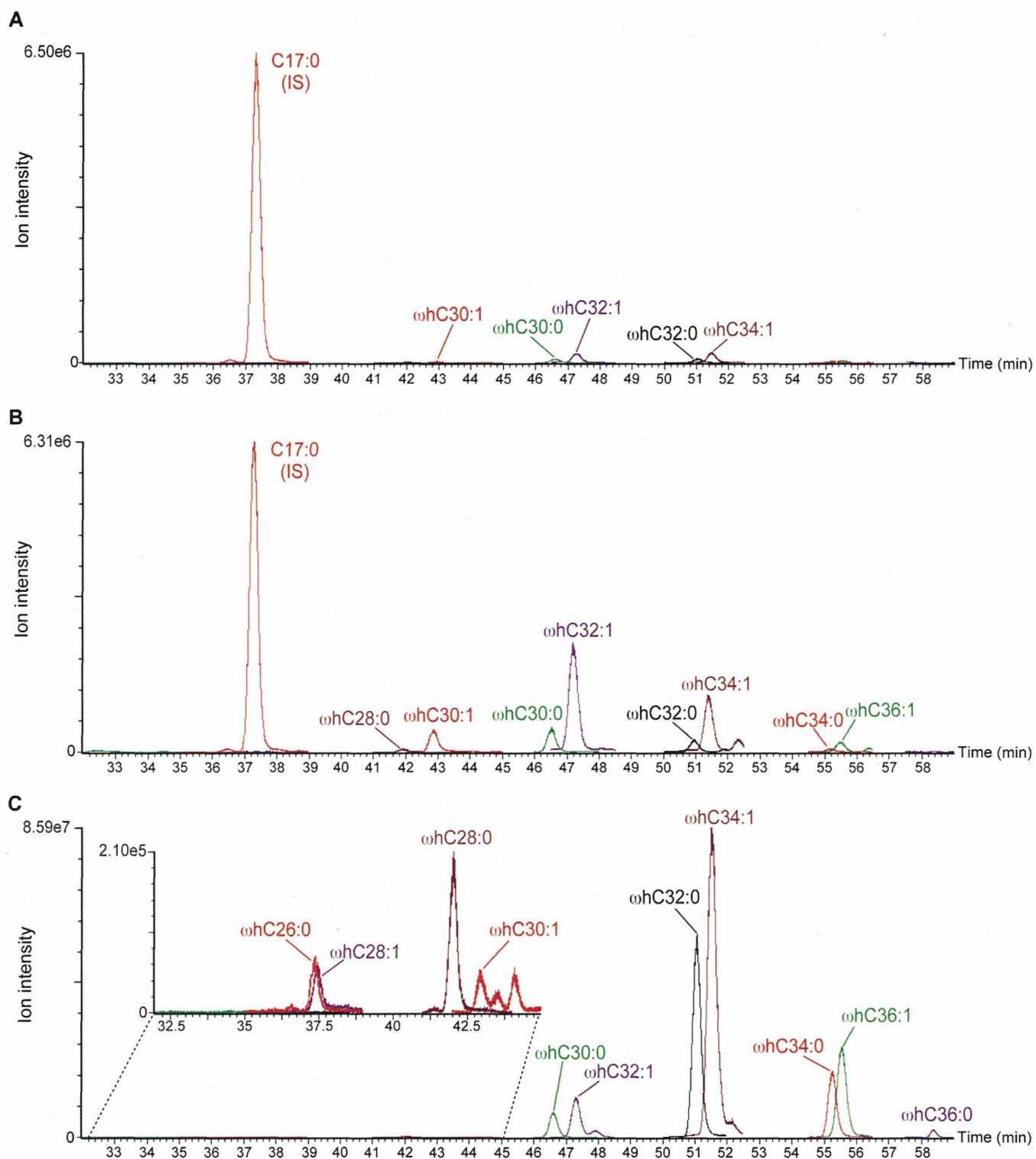


Fig. S5. MRM chromatogram of ω -hydroxyceramide species produced by CYP4F22. Lipids were extracted from HEK 293T transfected with pCE-puro 3xFLAG-ELOVL4 and pCE-puro 3xFLAG-CERS3, together with control vector (A) or pCE-puro 3xFLAG-CYP4F22 (B). EOS from mouse epidermis was treated with an alkali to liberate ω -hydroxyceramides (C). Lipids were subjected to UPLC/ESI-MS. Each ceramide was detected by MRM by setting the appropriate $[M+H]^+$ and $[M+H-H_2O]^+$ values at Q1 and m/z 264.2 at Q3. Each MRM peak was overlaid using MassLynx software. ω hC30:1, ω -hydroxyceramide with a chain length of C30:1. IS, internal control (C17:0 ceramide). The *Inset* in C shows an enlarged large view of the indicated area of the original chromatogram.